Surface Damage on Dental Implants with Release of Loose Particles after Insertion into Bone

Plinio Senna, DDS, MS;* Altair Antoninha Del Bel Cury, DDS, PhD;† Stephen Kates, MD;‡ Luiz Meirelles, DDS, MS, PhD§

ABSTRACT

Background: Modern dental implants present surface features of distinct dimensions that can be damaged during the insertion procedure into bone.

Purpose: The aims of this study were (1) to quantify by means of roughness parameters the surface damage caused by the insertion procedure of dental implants and (2) to investigate the presence of loose particles at the interface.

Materials and Methods: Three groups of dental implants representing different surface topographies were inserted in fresh cow rib bone blocks. The surface roughness was characterized by interferometry on the same area before and after the insertion. Scanning electron microscopy (SEM)–back-scattered electron detector (BSD) analysis was used to identify loose particles at the interface.

Results: The amplitude and hybrid roughness parameters of all three groups were lower after insertion. The surface presenting predominance of peaks (S_{sk} [skewness] > 0) associated to higher structures (height parameters) presented higher damage associated to more pronounced reduction of material volume. SEM-BSD images revealed loose titanium and aluminum particles at the interface mainly at the crestal cortical bone level.

Conclusions: Shearing forces during the insertion procedure alters the surface of dental implants. Loose metal particles can be generated at bone-implant interface especially around surfaces composed mainly by peaks and with increased height parameters.

KEY WORDS: bone, dental implants, surface properties, surface topography, titanium

INTRODUCTION

Oral rehabilitation with dental implants is a routine treatment modality for replacing missing teeth. The first generation of implants demonstrated an accepted bone crestal loss of <1 mm within the first year and <0.2 mm in the following years.[1] The development of new implant surfaces and designs together with improvement of the surgical/prosthetic hardware resulted in a reduction of bone loss associated to modern implants.[2] However, marginal bone loss is still a common finding poorly explained. Different theories suggest possible mechanisms such as the establishment of the biological width around a metal screw, occlusal overload, or peri-implantitis.

Successful implants will experience bone loss that usually takes place at a very early time points. Bone level changes calculated on radiographs taken from 1 to 54 weeks indicated that the change in height is limited to the first 6 weeks, and subsequent change is remarkably reduced.[3] Follow-up studies considering the implant placement as baseline for the analysis indicated a similar trend,[4,5] indicating that this initial bone loss first described by Branemark and colleagues[6] occurs much earlier than expected.

The surface of modern implants with enhanced roughness presents higher peaks that are more likely to

*PhD student, Department of Prosthodontics and Periodontology, Piracicaba Dental School, State University of Campinas, Brazil; †professor, Department of Prosthodontics and Periodontology, Piracicaba Dental School, State University of Campinas, Brazil; ‡professor, Department of Orthopaedics, University of Rochester, Rochester, NY, USA; §assistant professor, Division of Prosthodontics, Eastman Dental Center, University of Rochester, Rochester, NY, USA

Reprint requests: Luiz Meirelles, Division of Prosthodontics, Eastman Institute for Oral Health, University of Rochester, 625 Elmwood Avenue, Rochester, NY 14620;
e-mail: luiz_meirelles@urmc.rochester.edu

DOI 10.1111/cid.12167

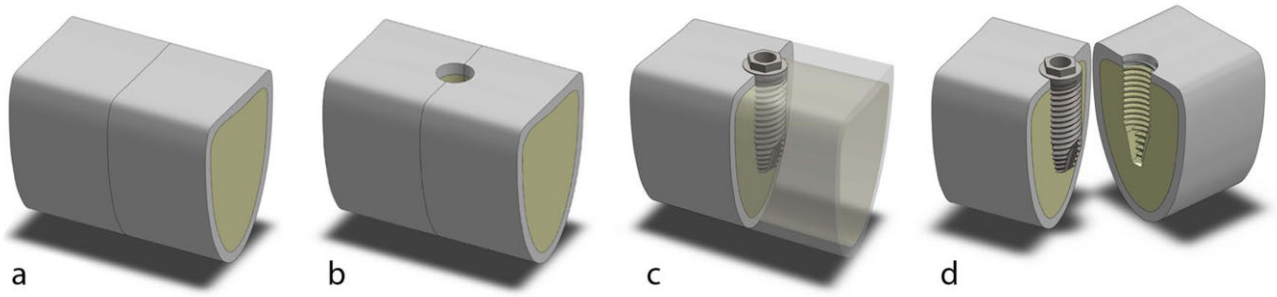

Figure 1 Cow rib bone blocks – 20 × 15 × 15 mm were cut transversely (A), and drilling was performed at the interface as recommended for dense bone (B). After the implants were fully inserted (C), the blocks were split, and the implant was assessed without any additional damage to the implant surface (D).

break and detach during the insertion procedure into bone. The quantitative characterization of surface topography of dental implants was introduced by Wennerberg and colleagues,[7] and the analysis of the roughness parameters before and after insertion is a reliable alternative to quantify the extent of wear.[8] Previous results indicated a change in surface topography of implants unscrewed after 12 weeks of healing in rabbits.[9] In vivo experiments indicated loose titanium particles in bone tissue around smooth-turned,[10,11] grit-blasted/acid-etched,[10] and plasma-sprayed implants.[10,12–14] More recently, soft tissue biopsies performed in patients after 6 months of implant installation detected Ti particles in the connective tissue facing the dental implants.[15,16]

The shear forces arising from the friction of self-tapping implants against the bone tissue produce a dynamic shifting of stresses on different locations along the implant related to the heterogeneity of bone tissue and the geometry of the implants.[17] Thus, dynamic localized spots are randomly created during insertion of the implants, generating particular areas of stress concentration that may compromise the integrity of the surface features and consequently release titanium particles in the bone tissue. Therefore, the aim of this study was to evaluate the surface damage to different dental implants caused by the insertion procedure itself and evaluate the generation of loose metal particles at the bone-implant interface.

MATERIALS AND METHODS

Fresh cow rib bone pieces were prepared and used immediately. Blocks measuring approximately 20 × 15 × 15 mm were cut with a diamond band saw (model C-40; Gryphon Corporation, Sylmar, CA, USA). Those blocks without 1.5 ± 0.5 mm thickness of cortical bone were excluded to keep the sample with similar thickness of human maxilla and mandible bones.[18] Next, each block was sectioned at the midline, and the two halves were bound tightly back together to the original configuration by a clamp to allow the insertion of the implant at the midline interface (Figure 1).

Cylindrical self-tapping threaded dental implants of similar dimensions and different surface topographies were selected ($n = 6$ per group): 4.0 × 10 mm TiUnite™ MkIII (TU; Nobel Biocare AB, Göteborg, Sweden), 4.0 × 11 mm OsseoSpeed™ TX (OS; Astra Tech AB, Mölndal, Sweden), and 4.1 × 10 mm SLActive® Bone Level (SL; Straumann AG, Waldenburg, Switzerland). TU surface features are produced by anodization process, whereas SL and OS surface features are produced by the combination of grit-blasting and acid-etching processes.[19]

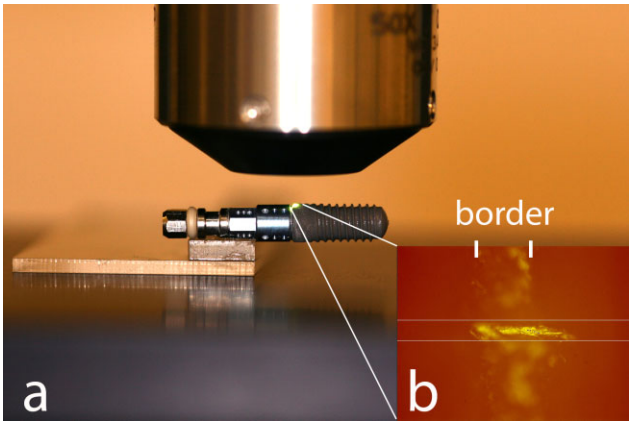

Figure 2 Implant positioning was obtained using the mount fixed to a slide (A). In addition, a scratch mark ensured the exact alignment to a predetermined mask set on the live display window of the software (B).

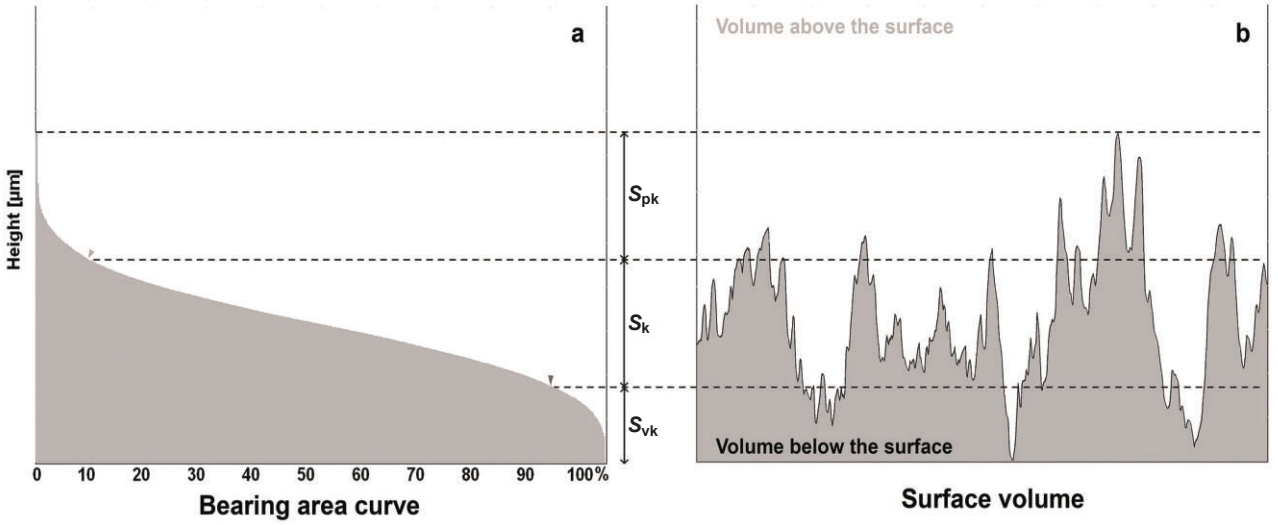

Figure 3 The functional parameters are determined from the bearing area ratio curve (A). S_{pk} corresponds to the peak height above the core roughness; S_k to the core roughness height (peak to valley) of the surface with the predominant peaks and valleys removed; and S_{vk} to valley depth below the core roughness. The sum of these parameters ($S_{vk} + S_k + S_{pk}$) determines the total structural height of the surface, and the material volume of surface features (Vm) comprises 100% of the surface material ratio (B) (S_{vk} = valley depth below the core roughness; S_k = core roughness height of the surface with the predominant peaks and valleys removed; S_{pk} = peak height above the core roughness).

The bone blocks were randomly divided, and drilling and implant insertion were performed at the interface of the two halves following each manufacturer's instructions with over copious irrigation. The implants were inserted at 25 rpm using the drilling unit (Elcomed SA-310; W&H Dentalwerk Bürmoos GmbH, Bürmoos, Austria). After the implants were fully inserted, the clamp was removed, and the blocks were split at the presectioned interface to retrieve the implant, which was easily removed without counter torque. This means that the removal procedure did not damage the implant surface. The implants were transferred to a plastic tube to be sonicated in purified water (30 minutes) and acetone (10 minutes) to remove residual bone debris from the surface. Acetone is an organic solvent known to be nonreactive to titanium and ceramics and commonly used to remove contaminants from titanium implants.

TABLE 1 Roughness Parameters of the Implant Groups before and after Insertion

Implant Parameter		TU	OS	SL
S_a (µm)	Before	1.05 ± 0.08	1.72 ± 0.14	2.28 ± 0.39
	After	0.95 ± 0.13	1.66 ± 0.14	2.08 ± 0.35
S_{dr} (%)	Before	33.66 ± 2.14	30.78 ± 5.05	82.68 ± 10.58
	After	27.45 ± 4.72	28.45 ± 3.80	59.48 ± 5.94
S_{vk} (µm)	Before	0.63 ± 0.11	2.63 ± 0.46	2.76 ± 0.80
	After	0.75 ± 0.22	2.51 ± 0.48	2.54 ± 0.69
S_k (µm)	Before	3.11 ± 0.35	5.38 ± 0.62	7.06 ± 1.20
	After	2.83 ± 0.50	5.16 ± 0.49	6.60 ± 1.10
S_{pk} (µm)	Before	1.70 ± 0.20	2.06 ± 0.52	3.44 ± 0.74
	After	1.53 ± 0.31	2.02 ± 0.48	2.75 ± 0.70
S_{sk}	Before	0.88 ± 0.18	-0.52 ± 0.30	0.19 ± 0.23
	After	0.56 ± 0.36	-0.49 ± 0.33	-0.01 ± 0.28

TU = TiUnite MkIII; OS = OsseoSpeed TX; SL = SLA Active Bone Level. S_a = average height deviation; S_{dr} = developed interfacial area ratio; S_{vk} = valley depth below the core roughness; S_k = core roughness height of the surface with the predominant peaks and valleys removed; S_{pk} = peak height above the core roughness; S_{sk} = degree of symmetry of the surface heights about the mean plane.

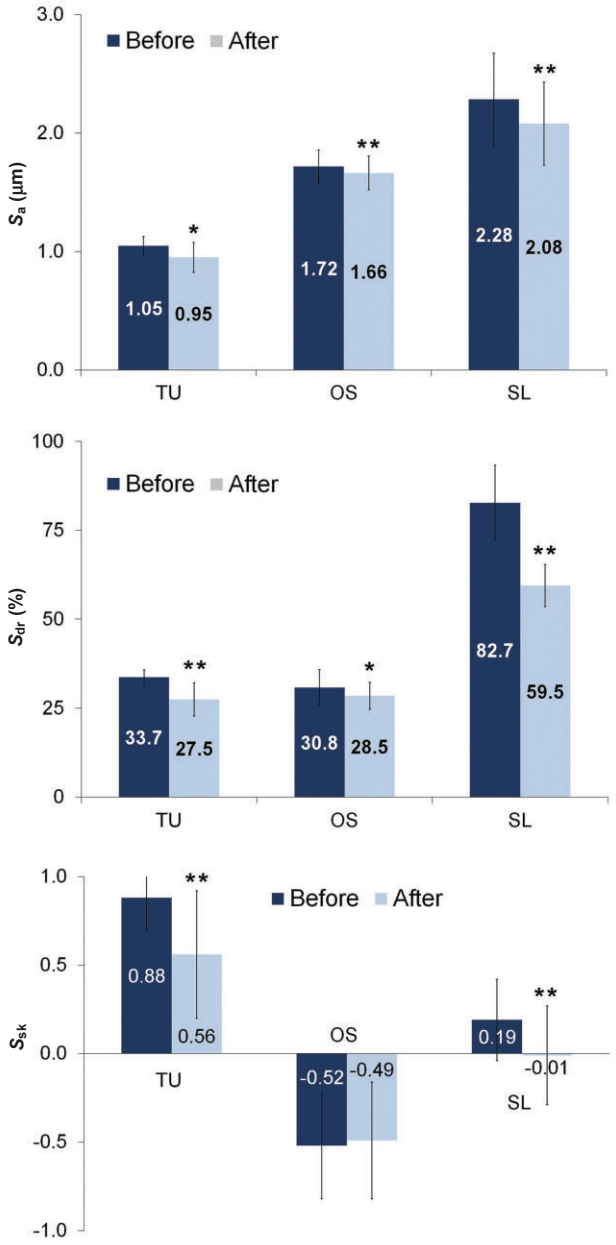

Figure 4 Surface roughness S_a, S_{dr}, and S_{sk} parameters (mean and SD) of the implants before and after insertion into bone (*$p < .05$ and **$p < .01$) (TU = TiUnite MkIII; OS = OsseoSpeed TX; SL = SLA Active Bone Level. S_a = average height deviation; S_{dr} = developed interfacial area ratio; S_{sk} = degree of symmetry of the surface heights about the mean plane).

The crest of all threads, including the microthreads on the neck of OS implants, was evaluated at the same regions before and after insertion by interferometry (New View 7300; Zygo, Middlefield, CT, USA) with objective ×50 and zoom factor of 0.5. An implant mount (SL implant) and a transfer (TU and OS) was fixed to slide to ensure that the implants were measured at the exact same spot before and after insertion. In addition, careful adjustment was obtained by matching a scratch mark to a predetermined rectangle mask set on the live display window of the software (MetroPro® version 9.1.2; Zygo) (Figure 2). Band pass Gaussian filter was used to remove errors of form and waviness.

The roughness parameters selected were calculated using Scanning Probe Image Processor software (version 5.1.8; Image Metrology A/S, Hørsholm, Denmark) and included

- amplitude parameters: S_a = average height deviation; S_{sk} = degree of symmetry of the surface heights about the mean plane (skewness)
- hybrid parameter: S_{dr} = developed interfacial area ratio
- functional parameters: S_{vk} = valley depth below the core roughness; S_k = core roughness height of the surface with the predominant peaks and valleys removed; S_{pk} = peak height above the core roughness (Figure 3A)

In addition, the peak density and the material volume (Vm) correspondent to 100% of the surface features (Figure 3B) were calculated using MetroPro software. The average difference in Vm ($Vm_{intial} - Vm_{final}$) calculated by the interferometer was then correlated with the total surface area of the implants to estimate the total volume of particles detached from the surface considering a uniform damage along the entire implant. For this, one implant of each group was subjected to a micro computed

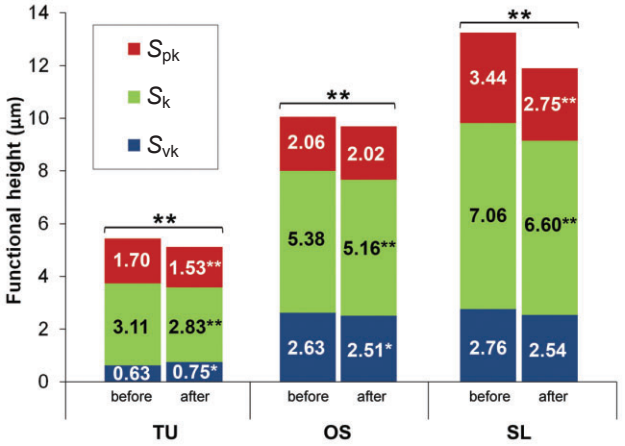

Figure 5 The surface functional height ($S_{vk} + S_k + S_{pk}$) of implants before and after insertion into bone (*$p < .05$ and **$p < .01$) (TU = TiUnite MkIII; OS = OsseoSpeed TX; SL = SLA Active Bone Level. S_{vk} = valley depth below the core roughness; S_k = core roughness height of the surface with the predominant peaks and valleys removed; S_{pk} = peak height above the core roughness).

tomography (micro-CT) scanning (vivaCT 40; Scanco USA Inc., Wayne, PA, USA) to determine the total surface area of the implant, which revealed 173.31, 176.71, and 158.22 mm^2 for TU, OS, and SL groups. From the total volume estimated, the mass of particles was calculated considering the density of titanium dioxide as 4.23 g/cm^3.

Scanning electron microscopy (SEM) images of the implants before and after insertion were performed (Zeiss Auriga SEM/FIB, Oberkochen, Germany) at different magnifications associated to back-scattered electron detector (BSD) at 20 kV with a resolution of <5 nm and energy-dispersive x-ray spectroscopy (EDS). To detect the presence of loose titanium particles along the bone implantation sites, the bone blocks were dried at 37°C for 48 hours after implant removal and evaluated by BSD/EDS. Remaining debris on the bone surface related to the insertion procedure were removed prior to SEM-EDS with a jet spray to avoid unstable structures that would compromise the analysis and contaminate the electron microscope vacuum chamber.

The roughness parameters, peak density, and Vm data before and after implant insertion were analyzed by paired *t*-test ($\alpha = 0.05$) (*SPSS* Statistics 20; IBM Corporation, Armonk, NY, USA).

RESULTS

Implant insertion torque never exceeded the maximum value recommended by the manufacturer. Average insertion torque (Ncm) of 40.4(2.0), 35.2(3.1), and 36.5(2.5) was calculated for TU, OS, and SL implants, respectively.

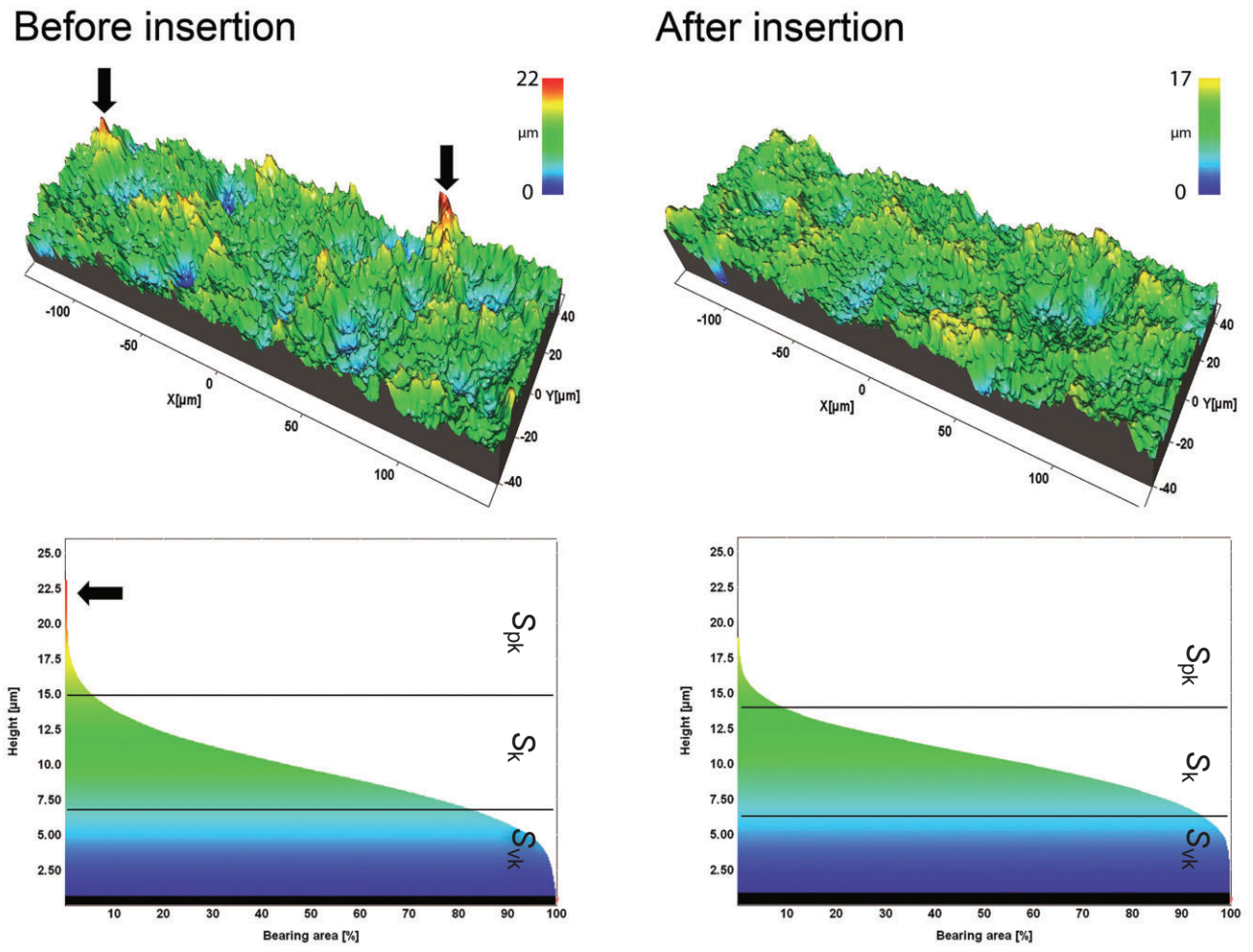

Figure 6 The surface topography of a thread of SL implants (SLA Active, Bone Level) before and after insertion into bone and respective bearing area curves. Summits (red peaks) were visually less prevalent after implant insertion (S_{vk} = valley depth below the core roughness; S_k = core roughness height of the surface with the predominant peaks and valleys removed; S_{pk} = peak height above the core roughness).

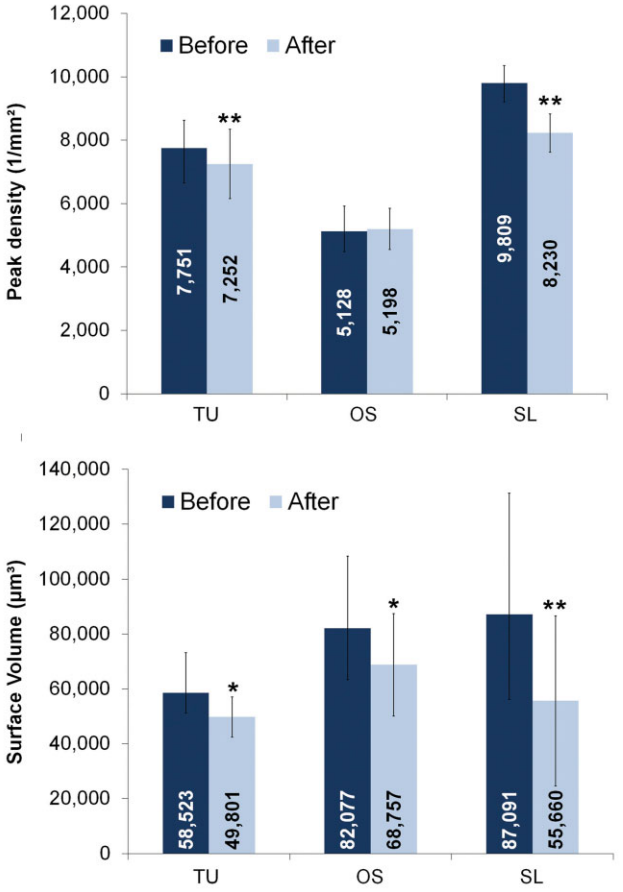

Figure 7 Peak density and surface volume (mean and SD) of implants before and after insertion into bone (*$p < .05$ and **$p < .01$).

The results are summarized in Table 1. The average height deviation (S_a) of the TU, OS, and SL implants demonstrated a reduction of 0.1, 0.06, and 0.2 µm after insertion (Figure 4). The degree of symmetry measured by the S_{sk} showed a predominance of peaks above the mean plane to TU and SL ($S_{sk} > 0$) implants. After insertion, the reduction on the S_{sk} values of TU and SL implants indicates a shift on the height profile toward a more symmetrical distribution explained by loss of the peaks. In contrast, S_{sk} initial negative value for OS implants reveals that the initial surface was composed predominantly of valleys, and the similar values before and after insertion indicated that height distribution was not affected (Figure 4). The change of the developed interfacial area ratio (S_{dr}) values followed the same pattern as observed for the average height deviation (S_a) values; higher reduction to SL (Δ 23.2%) followed by TU (Δ 6.2%) and OS (Δ 2.3%).

TU implants exhibited slightly deeper extreme valleys (S_{vk}) after insertion coupled to a reduction of both the core roughness (S_k) and extreme peaks (S_{pk}) of 0.28 and 0.17 µm that resulted in an overall height reduction ($S_{vk} + S_k + S_{pk}$) of 0.33 µm. OS implants exhibited a reduction of the S_{vk} and S_k of 0.12 and 0.22 µm, where the S_{pk} was similar after insertion, resulting on an overall reduction of 0.33 µm. Although the OS and SL undergo similar surface modifications, the functional parameters modification indicated a different behavior under stress. SL implants were mainly affected on the extreme peaks, with a reduction of the S_{pk} of 0.69 µm, whereas the core roughness and extreme valleys showed a reduction of 0.45 and 0.22 µm that resulted in an overall height reduction of 1.36 µm (Figure 5). An example of an SL implant measurement of the same thread before and after shows that the extreme peaks were predominantly affected compared with the core roughness and extreme valleys (Figure 6).

TU, OS, and SL groups demonstrated an average Vm reduction of the volume at the crest of the threads of 8,723, 13,320, and 31,431 µm^3 (Figure 7). This corresponded to 0.06, 0.14, and 0.54 mg of released particles from TU, OS, and SL implants. The threads were randomly damaged during insertion, even in the same implant group, as observed by the broad range of Vm reduction considering each thread (Figure 8). Although some threads were minimally affected, others threads of OS and SL implants exhibited the highest structural height reduction (Figure 9).

After insertion, SEM images of TU implants showed chipping of the porous structures along the surface associated with cracks on the base of the anodized layer (Figure 10A). Also, delamination was seen at the sharp edges of the cutting threads with exposure of bulk

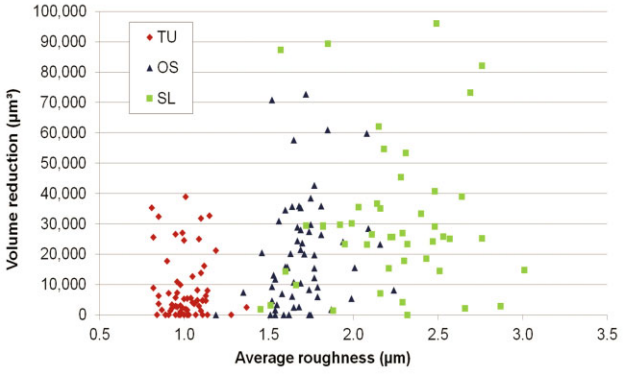

Figure 8 The surface volume reduction after implant insertion according to the average roughness (S_a) computed at the crest of all threads of TU, OS, and SL groups (TU = TiUnite MkIII; OS = OsseoSpeed TX; SL = SLA Active Bone Level).

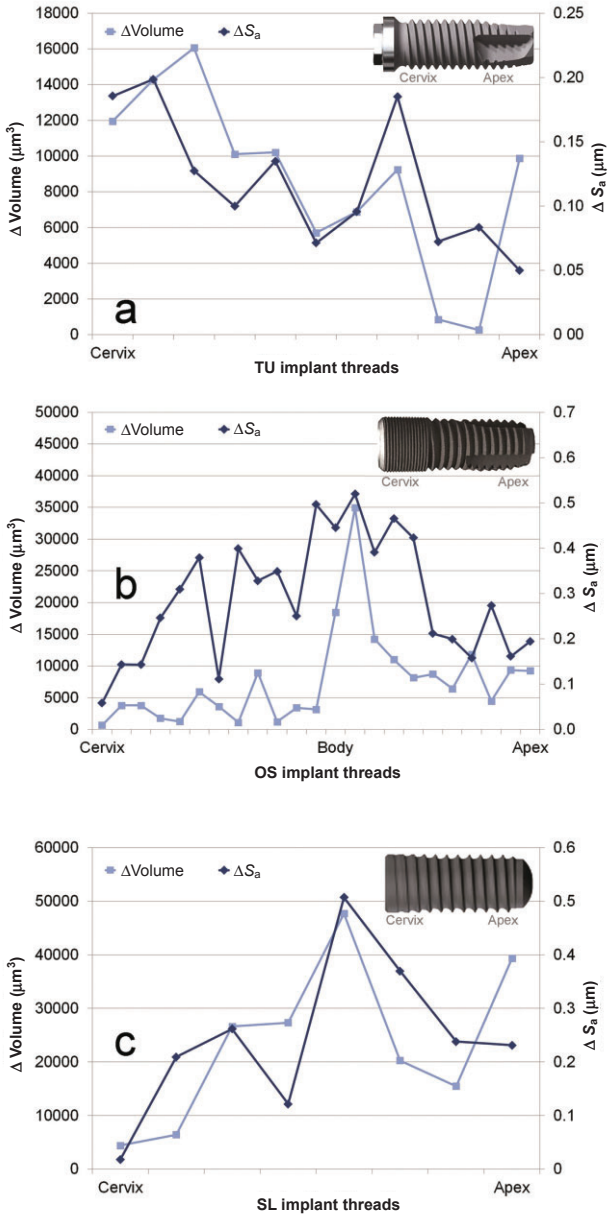

Figure 9 The average height deviation (S_a) and surface material volume (Vm) reduction on each individual thread after insertion along TU (A), OS (B), and SL (C) implants (TU = TiUnite MkIII; OS = OsseoSpeed TX; SL = SLA Active Bone Level).

titanium (Figure 10B). The sharp peaks present initially at the grit-blasted and acid-etched implants (OS and SL) were less prominent or completely removed after insertion, resulting in flattened smooth areas (Figures 11 and 12). The BSD/EDS evaluation revealed presence of titanium debris along the implantation site of bone blocks separated from TU, SL, and OS implants (Figures 10, 11, and 12). Loose titanium particles of 10 nm to 20 µm were seen on the implantation sites, concentrated mainly around the cortical bone layer, especially at the microthread region of OS implants. Bone blocks adjacent to SL implants revealed Al particles (Figure 13).

DISCUSSION

Pilot tests were performed to ensure that the maximum insertion torque for the implant groups never exceeded the values recommended by each company. This critical step was important to simulate an ideal placement and to ensure that any damage to the surface was not related to implant overtorque. In addition, secondary damage was achieved by cutting the bone blocks in half prior to implant insertion, allowing an easy removal of the implant by separating the block in two pieces. It would be hard to estimate any further damage related to the attempt to remove the implant by unscrewing or cutting the bone block with the implant already installed. Thus, any change in surface topography of the implants evaluated in the present study is restricted to the actual insertion procedure and does resemble the clinical scenario.

The S_a is the most used roughness parameter used to characterize implant surfaces and indicated that the height of the structures was more affected on the rougher SL implants. The higher surface alteration to the rougher SL implant was further confirmed by the more pronounced reduction of the hybrid S_{dr} parameter and the more pronounced reduction of surface volume compared with TU and OS implants. However, the reason was not clear why both blasted and acid-etched implants (OS and SL) experienced such clear distinguished alteration after insertion.

The amplitude and hybrid parameters demonstrated change in the surface topography of all three groups, but they are not sensitive to indicate the pattern of wear within the surface. To complement the amplitude and hybrid parameters, functional parameters are an alternative to separate the features within the surface. Surface features are separated as extreme peaks (S_{pk}), core (S_k), and extreme valleys (S_{vk}), providing a tool to inspect the damage at different levels.[8] This approach proved to be a valuable technique to analyze different surfaces of dental implants and identify where the damage occurred. SL rougher implant demonstrated a pronounced reduction of S_{pk} and decreased S_k after insertion, whereas the S_{vk} was not statistically different. In contrast to SL implants, OS implants demonstrated a reduction of the core roughness (S_k) and the deep valleys (S_{vk}), whereas the extreme peaks were not affected (Figure 5).

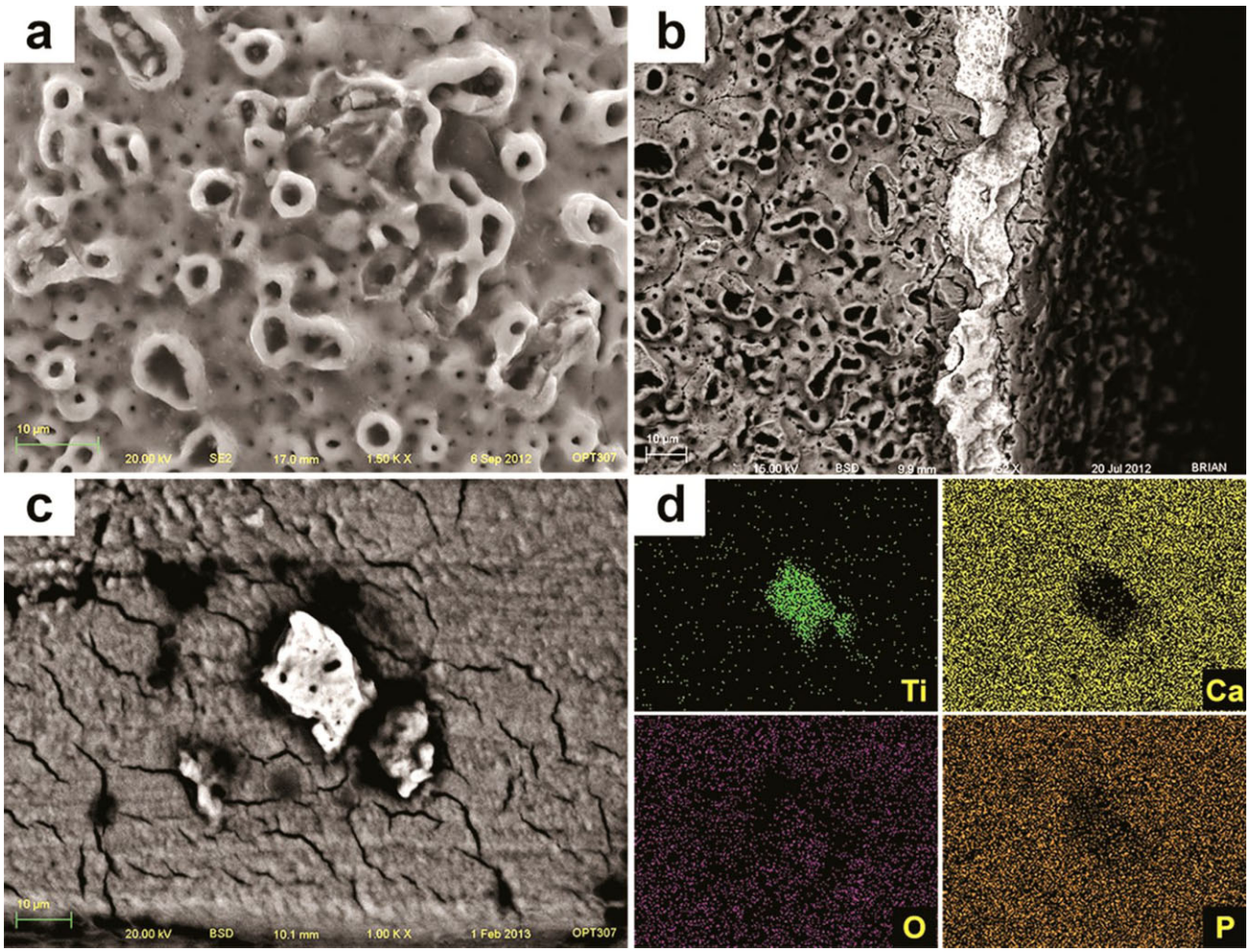

Figure 10 Scanning electron microscopy (SEM) image of TiUnite MkIII (TU) implant after insertion into bone revealed chipping of the more extreme porous (A) and cracks on the oxide layer associated to loss of entire oxide layer at the cutting edge with exposure of the bulk Ti (B). Along the implantation sites, pieces of the oxide layer were identified by SEM-back-scattered electron detector (BSD) (C), and their Ti content was shown by EDS mapping of the surface (D).

SL and OS implants are treated by the same surface modification techniques (blasting and acid etching), but the two implants have a clear different height distribution. OS implants exhibit a surface predominantly formed by structures below the mean plane ($S_{sk} < 0$), whereas the SL implants have a slight asymmetry toward structures above the mean plane ($S_{sk} > 0$), explaining the unexpected similar S_{pk} values before and after insertion for the OS implants and overall higher surface alteration to the rougher and positively skewed SL implants. The chipping of the oxide layer of the anodized TU implants at some threads explains the discrete increase of the S_{vk}, resulting in some deeper structures combined to the expected wear of the S_{pk} extreme peaks extending to the S_k core roughness. The direct analysis of the peak density values corroborated with the alterations detected by the roughness parameters. Positively skewed surfaces of TU and SL implants demonstrated a significant reduction of the number of peaks after insertion, whereas the negatively skewed OS implants revealed similar values before and after insertion (Figure 7). It is clear from the present results that the negative height distribution associated to a lower S_{dr} reduced the overall modification of the OS implants despite the higher S_a value compared with TU implants. In addition, the combination of higher S_a and S_{dr} values associated to a positive height distribution on SL implants determines the more pronounced volume reduction compared with TU and OS implants.

The present study showed that the insertion procedure itself is able to release up to 0.5 mg of particles at implant-bone interface. Previous studies reported

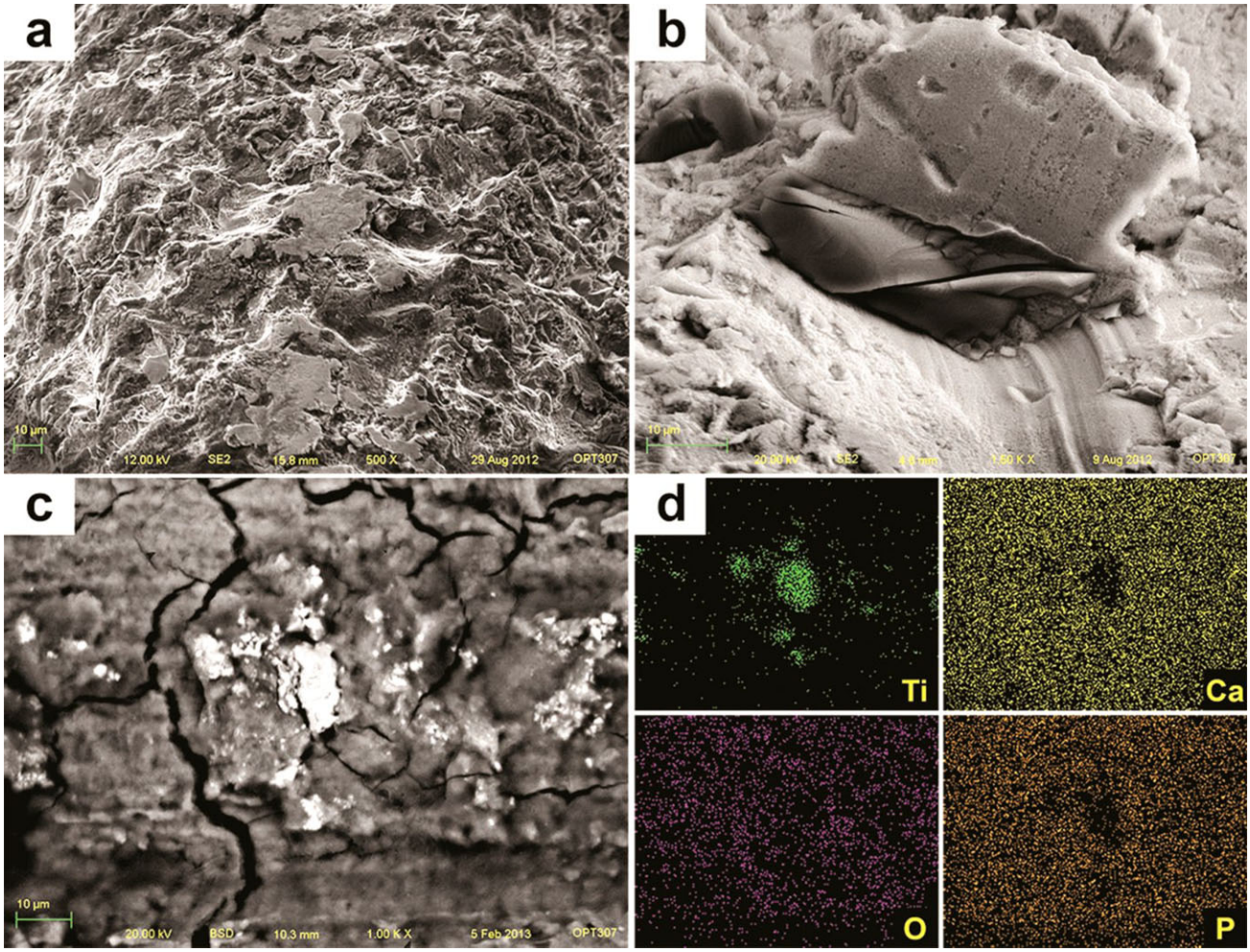

Figure 11 SEM image of OS implant after insertion into bone revealed sharp peaks less prominent or completely removed, resulting in flattened smooth areas after implant insertion (A). Also, the TiO_2 grit-particles (dark and smooth) embedded into the surface (B) were less prevalent after insertion. Along the implantation sites, particles were identified by scanning electron microscopy–back-scattered electron detector (SEM-BSD) (C), and their Ti content was shown by energy-dispersive x-ray spectroscopy (EDS) mapping of the surface (D).

that aseptic osteolysis was induced by 0.2[20] to 3.0 mg[21] of loose titanium particles, showing extensive and nonuniform osteoclastic activity with a resorbed bone area 8%[20] to 35%[21] higher than the control sites without particles at 7 to 10 days, respectively. However, the evaluation of bone after 16 weeks failed to show any clear ongoing resorption, and few reminiscent particles were detected.[22] Therefore, it seems that the aseptic osteolytic response to titanium particles is transient dependent on the presence of the particles. A recent follow-up with unusual radiographic protocol demonstrated a similar trend around dental implants. Vandeweghe and colleagues[3] based on a detailed radiographic regimen evaluated crestal bone changes as early as 1 week. The results demonstrated that 0.95 mm (75%) of bone loss during the first year occurred within the first 6 weeks, and a steady decrease of 0.1 mm was observed at 3, 6, and 12 months. Other studies that considered the implant placement as baseline for crestal bone height evaluation indicated the same trend: a higher ratio of bone loss at 3- and 6-month intervals compared with 1 year follow-up.[4,5]

A prolonged imbalance on bone remodeling related to the loose titanium particles is not expected in healthy subjects. After 16 weeks, no clear active bone resorption was observed in rabbits loaded with Ti-6Al-4V despite the presence of few reminiscent particles.[22] This finding is in agreement with the crestal bone height changes observed in follow-up studies where a highest percentage of bone loss occurred

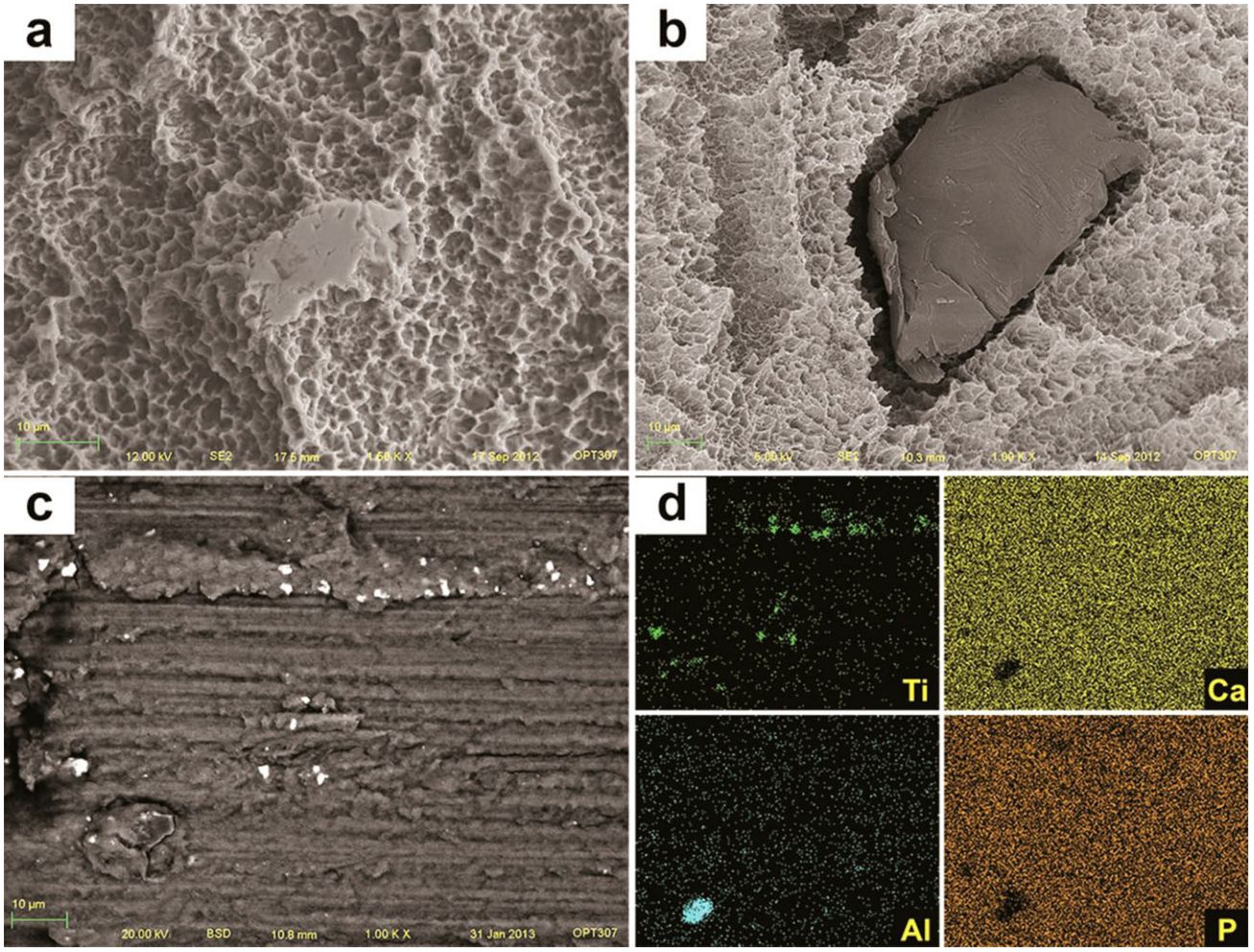

Figure 12 Scanning electron microscopy (SEM) image of SLActive Bone Level (SL) implant after insertion into bone revealed sharp peaks less prominent or completely removed, resulting in flattened smooth areas after implant insertion (A). Also, the alumina grit-particles (dark and smooth) embedded into the surface (B) were less prevalent after insertion. Along the implantation sites, particles were identified by SEM–back-scattered electron detector (BSD) (C), and their Ti and Al content was shown by energy-dispersive x-ray spectroscopy (EDS) mapping of the surface (D).

during the first 3 months, and fairly stable values were observed thereafter.[3,4]

The generation of loose particles at the interface during insertion has been previously described, and increased number of particles was associated to rougher implants[11]and may contribute to the early marginal bone loss around well-integrated dental implants. The great majority of the particles is phagocytised by macrophages and removed from the implant-bone interface, preventing a permanent bone resorption. The final destination of such particles was investigated in minipigs. After 5 months, no particles were detected at the bone-implant interface and were found in the lungs, kidneys, and liver.[11] This indicates the possibility of migration of these particles released from the surface of dental implants from the jaw bone to other organs.

CONCLUSION

Surface damage was observed on all three implant groups. The combined enhanced S_a and positive S_{sk} values of SL implants resulted in more surface damage during the insertion procedure. Loose titanium particles of different sizes were detected embedded in the bone walls as a result of wear of the surface features. Future experiments should elucidate the clinical relevance of such particles on peri-implant tissue response.

ACKNOWLEDGMENTS

This work was supported by National Institutes of Health PHS award P30 AR61307. The authors would like to thank to the São Paulo Research Foundation (FAPESP #2011/23269-0) for the scholarship granted to P.S.

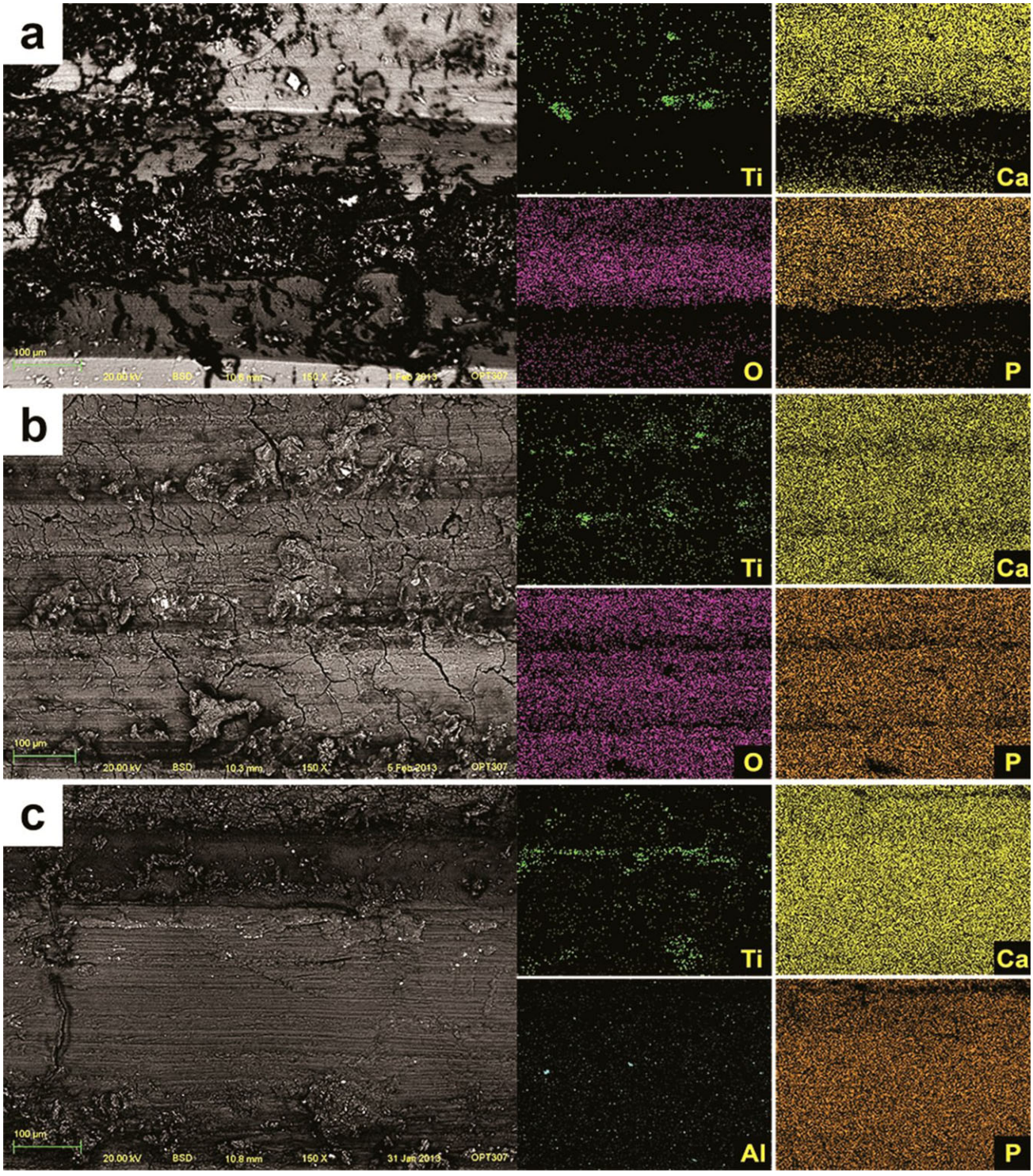

Figure 13 Scanning electron microscopy–back-scattered electron detector (SEM-BSD) images of the implantation sites showed titanium loose particles (white shiny spots) along all implantation sites after removal of TiUnite MkIII (TU) (A), OsseoSpeed TX (OS) (B), and SLActive Bone Level (SL) implants (C). The elemental content of those particles (Ti for TU and OS, and Ti and Al for SL implants) was confirmed by the energy-dispersive x-ray spectroscopy (EDS) mapping of the surface.

REFERENCES

1. Albrektsson T, Zarb G, Worthington P, Eriksson AR. The long-term efficacy of currently used dental implants: a review and proposed criteria of success. Int J Oral Maxillofac Implants 1986; 1:11–25.
2. Laurell L, Lundgren D. Marginal bone level changes at dental implants after 5 years in function: a meta-analysis. Clin Implant Dent Relat Res 2011; 13:19–28.
3. Vandeweghe S, Cosyn J, Thevissen E, Van den Berghe L, De Bruyn H. A 1-year prospective study on Co-Axis implants immediately loaded with a full ceramic crown. Clin Implant Dent Relat Res 2012; 14(Suppl 1):e126–e138.
4. Collaert B, Wijnen L, De Bruyn H. A 2-year prospective study on immediate loading with fluoride-modified implants in the edentulous mandible. Clin Oral Implants Res 2011; 22:1111–1116.
5. Hammerle CH, Jung RE, Sanz M, Chen S, Martin WC, Jackowski J. Submerged and transmucosal healing yield the same clinical outcomes with two-piece implants in the anterior maxilla and mandible: interim 1-year results of a randomized, controlled clinical trial. Clin Oral Implants Res 2012; 23:211–219.
6. Branemark PI, Hansson BO, Adell R, et al. Osseointegrated implants in the treatment of the edentulous jaw. Experience from a 10-year period. Scand J Plast Reconstr Surg Suppl 1977; 16:1–132.
7. Wennerberg A, Albrektsson T, Ulrich H, Krol JJ. An optical 3-Dimensional technique for topographical descriptions of surgical implants. J Biomed Eng 1992; 14:412–418.
8. Dong WP, Stout KJ. An integrated approach to the characterization of surface wear .1. qualitative characterization. Wear 1995; 181:700–716.
9. Wennerberg A, Albrektsson T, Andersson B. An animal study of Cp Titanium screws with different surface topographies. J. Mater. Sci. - Mater. Med. 1995; 6:302–309.
10. Meyer U, Buhner M, Buchter A, Kruse-Losler B, Stamm T, Wiesmann HP. Fast element mapping of titanium wear around implants of different surface structures. Clin Oral Implants Res 2006; 17:206–211.
11. Schliephake H, Reiss G, Urban R, Neukam FW, Guckel S. Metal release from titanium fixtures during placement in the mandible: an experimental study. Int J Oral Maxillofac Implants 1993; 8:502–511.
12. Franchi M, Bacchelli B, Martini D, et al. Early detachment of titanium particles from various different surfaces of endosseous dental implants. Biomaterials 2004; 25:2239–2246.
13. Franchi M, Orsini E, Martini D, et al. Destination of titanium particles detached from titanium plasma sprayed implants. Micron 2007; 38:618–625.
14. Martini D, Fini M, Franchi M, et al. Detachment of titanium and fluorohydroxyapatite particles in unloaded endosseous implants. Biomaterials 2003; 24:1309–1316.
15. Flatebo RS, Hol PJ, Leknes KN, Kosler J, Lie SA, Gjerdet NR. Mapping of titanium particles in peri-implant oral mucosa by laser ablation inductively coupled plasma mass spectrometry and high-resolution optical darkfield microscopy. J Oral Pathol Med 2011; 40:412–420.
16. Flatebo RS, Johannessen AC, Gronningsaeter AG, et al. Host response to titanium dental implant placement evaluated in a human oral model. J Periodontol 2006; 77: 1201–1210.
17. Guan H, RCv S, Johnson NW, Loo Y-C. Dynamic modelling and simulation of dental implant insertion process-A finite element study. Finite Elem Anal Design 2011; 47:886–897.
18. Katranji A, Misch K, Wang HL. Cortical bone thickness in dentate and edentulous human cadavers. J Periodontol 2007; 78:874–878.
19. Wennerberg A, Albrektsson T. On implant surfaces: a review of current knowledge and opinions. Int J Oral Maxillofac Implants 2010; 25:63–74.
20. Kaar SG, Ragab AA, Kaye SJ, et al. Rapid repair of titanium particle-induced osteolysis is dramatically reduced in aged mice. J Orthop Res 2001; 19:171–178.
21. Shin DK, Kim MH, Lee SH, Kim TH, Kim SY. Inhibitory effects of luteolin on titanium particle-induced osteolysis in a mouse model. Acta Biomater 2012; 8:3524–3531.
22. Goodman SB, Davidson JA, Song Y, Martial N, Fornasier VL. Histomorphological reaction of bone to different concentrations of phagocytosable particles of high-density polyethylene and Ti-6Al-4V alloy in vivo. Biomaterials 1996; 17: 1943–1947.